Earthquakes and Structures, *Vol. 12, No. 1 (2017) 35-45*
DOI: https://doi.org/10.12989/eas.2017.12.1.035

Effect of seismic pounding on buildings isolated by triple friction pendulum bearing

Gholamreza Ghodrati Amiri*[1], Ayoub Shakouri[2a], Sajad Veismoradi[2b] and Pejman Namiranian[2c]

[1]*Center of Excellence for Fundamental Studies in Structural Engineering, School of Civil Engineering, Iran University of Science and Technology, Tehran, Iran*
[2]*School of Civil Engineering, Iran University of Science and Technology, Tehran, Iran*

(Received September 2, 2016, Revised October 31, 2016, Accepted November 4, 2016)

Abstract. The current paper investigates the effect of the seismic pounding of neighboring buildings on the response of structures isolated by Triple Friction Pendulum Bearing (TFPB). To this end, a symmetric three-dimensional single story building is modeled for analysis with two specified levels of top deck and base deck, to capture the seismic response of the base isolators and building's roof. Linear elastic springs with different level of gaps are employed to calculate the impact between the buildings. Nonlinear Dynamic Time History Analyses (NDTHA) are conducted for seismic evaluation. Also, five different sizes with four different sets of friction coefficients are assumed for base isolators to cover a whole range of base isolation systems with various geometry configurations and fundamental period. The results are investigated in terms of base shear, buildings' drift and top deck acceleration of the superstructure. The results also indicate the profound effect of the stiffness of the adjacent buildings on the value of the impact they impose to the superstructure. Also, in situations of potential pounding, the increment of the fundamental period of the TFPB base isolator could intensify the impact force up to nearly five-fold.

Keywords: triple friction pendulum bearing; impact; nonlinear dynamic time history analysis; base isolation; pounding

1. Introduction

Post-earthquake damage inspections have revealed the vulnerability of structural buildings to seismic induced pounding. In this regard, due to small separation distance between two adjacent structures, the buildings are susceptible to collide against each other during the seismic excitations. The problem tends to become more substantial in the case of large metropolitan areas where buildings are closely constructed with insufficient gap. Investigation of the past earthquakes illustrated several cases of pounding damages in buildings, ranging from minor local to more severe damage that could even initiate structural collapse (See for example, Bertero 1987, Kasai and Maison 1997, Cole *et al.* 2011, Takewaki *et al.* 2011). The results of Anagnostopoulos (1988) indicated that the larger differences in the masses of the two adjacent buildings, would make the pounding effects more detrimental for the lighter frame. Furthermore, some of the studies show that higher level of damage could occur in interstory pounding case of the buildings with unequal heights (Bertero 1987, Karayannis and Favvata 2005a). The most important issue in the inter-story pounding is related to the local damage imposed on the external column of the taller building which suffers the impact from the upper floor slab of the adjacent shorter and stiffer structure (Karayannis and Favvata 2005b). Besides being dependent on the structural characteristics of the buildings, other factors such as soil-structure interaction could also affect the seismic pounding significantly, especially for lighter and more flexible structures (Mahmoud *et al.* 2013).

To minimize or preclude the seismic pounding phenomenon, several measures are specified. Undoubtedly, the best and simplest mitigation measure is the provision of sufficiently wide gap between buildings to avoid any impact incidences. However, providing such a separation space tends to be difficult in high-density populated areas with maximum land usage requirements. Also, such an action is not applicable in case of retrofitting the existing structures. Other solutions include using permanent connections between the adjacent buildings (Raheem 2014), utilizing shock absorbing materials to fill the gap between the two buildings (Polycarpou and Komodromos 2011, Polycarpou *et al.* 2013), or adding the energy absorbing dampers in case of base isolated buildings to prevent any seismic pounding damage (Rawlinson *et al.* 2015). However, most of these proposed solutions are in their early stages of development and difficult to apply, specifically in case of many buildings in metropolitan cities which are already constructed in very close distance to each other and could suffer from possible poundings in the upcoming earthquakes. For these reasons,

*Corresponding author, Professor
E-mail: Ghodrati@iust.ac.ir
[a]Ph.D. Student
E-mail: m_shakoori@civileng.iust.ac.ir
[b]MSc.
E-mail: veysmoradi@alumni.iust.ac.ir
[c]Ph.D.
E-mail: namiranian@alumni.iust.ac.ir

 ISSN: 2092-7614 (Print), 2092-7622 (Online)

it has been widely accepted that the pounding phenomenon should be investigated to determine the vulnerability of current buildings against seismic impact.

Seismic isolation technology is widely accepted approach for reducing the seismic loads in buildings which decouples the superstructure of concern by increasing the flexibility of the system beyond the predominant periods of ground motions and additional energy dissipation as well as damping ratio. The main objective of using a base isolator is to protect the superstructure from accumulation of inelastic demands in the structural parts of the building. However, it is expected that isolated buildings experience large horizontal displacement during seismic excitations, especially in case of near-fault ground motions with pulse-like nature. As a result, the seismic pounding phenomenon of the buildings with small gap distance becomes more detrimental for isolated frames, which exhibit quite different dynamic behavior than the same regular fixed-supported frames. It should be mentioned that insufficient seismic gap could also negatively affect the performance of the base isolation systems which necessitates the investigation for isolated buildings even more.

As compared to extensive research on the pounding of conventional frames with fixed base, a few studies have been carried out for seismic pounding of base-isolated buildings. Malhotra (1997) was among the first researchers who investigated the effect of pounding in isolated structures and demonstrated that the base shear generated by impact can be higher than the total weight of the building; also the increase in the stiffness of the retaining wall or adjacent structures could directly increase the base shear force. Matsagar and Jangid (2003) investigated the pounding effects on a MDOF system and concluded that the effects of impact tend to intensify as the flexibility and story number of the structures increase. Komodromos *et al.* (2007) investigated the pounding response of multistory isolated buildings against the surrounding moat wall and revealed the more severe interstory deflections due to impact in upper story levels of the superstructure. Polycarpou and Komodromos (2010) performed numerical simulations to investigate the effects of separation distance and earthquake characteristics on seismic poundings of isolated buildings. Their results have revealed that even if a sufficient distance is provided for the isolated buildings, this cannot ensure the safety of the buildings against seismic pounding since the horizontal deformation of the adjacent buildings plus large relative displacement of the superstructure may exceed the gap distance, especially in upper story levels. They also indicated that the effects of pounding are more detrimental when the adjacent structures are in resonance with the earthquake ground motions. Masroor and Mosqueda (2012) utilized a quarter scale three-story frame isolated with friction pendulum bearings to experimentally investigate the pounding effects on the base-isolated buildings. They demonstrated that the contact forces imposed during the seismic pounding can result in yielding of superstructure and enhance the response acceleration at all story levels. Khoshnoudian and Hemmati (2014) investigated the seismic pounding of buildings with Double Concave Friction Pendulum (DCFP) Bearing by considering the tri-linear and bi-linear behavior of isolator. Their results exhibited up to 48% decrease in the base shear of tri-linear DCFP bearing. However, the tri-linear DCFP causes larger displacements in sliding surfaces.

Although the above described researches on seismic pounding of the base isolated buildings provide some basic information regarding the performance of isolated buildings during the seismic-induced poundings, there is still a need for further investigation, taking into account the behavior of new base-isolation systems. Focusing on the newly introduced Triple Friction Pendulum Bearing (TFPB) base isolation systems, in this work, the effect of earthquake pounding on the seismic behavior of the base-isolated buildings by TFPB system is investigated. Five different sizes of TFPB isolators are modelled and four different cases are considered regarding the friction coefficient parameters for each size of the isolator (20 cases in total), covering a whole range of geometric configuration and fundamental period for the TFPBs. The effect of certain parameters such as separation distance, stiffness of impact element and behavior of TFPBs are taken into consideration.

2. Triple Friction Pendulum Bearing: a brief review

Triple Friction Pendulum Bearing (TFPB) is a novel base isolation system with four concave surfaces separated by an internal rigid slider which can represent greater maximum displacement, compared to similar sized single pendulum bearings. All of the four surfaces are coated with non-metallic sliding material with a friction coefficient as depicted in Fig. 1 (Dao *et al.* 2013). The inner slider slides between two slide plates with spherical surfaces with radius R2 and R3, which can slide between top and bottom concave plates. The isolator is designed in a distinguished manner that during the course of motion, the internal segments of the base isolator induce sliding to occur in different combination of surfaces, thereby providing changes in stiffness and damping at desired displacement demands (Fenz 2008). Beside adjusting the design parameters to reach the desired performance states on different levels of seismic actions, the friction coefficient on each surface can also be changed in a continuous manner such as Variable friction systems (Namiranian *et al.* 2016) to provide the engineers with a variety of parameters to fulfil their design needs. The isolator has already been utilized by engineers to protect the important buildings from strong earthquakes (take the Mills-Peninsula Hospital in California as an example which utilizes 176 TFPBs to keep the hospital operational, even after strong earthquakes). According to Fenz and Constantinou (2008a, b), the isolator presents five different stages (regime of motion) in its force-displacement hysteresis behavior as depicted in Fig. 2:

Stage 1: Sliding occurs on surface 2 and 3 with high stiffness and low friction which demonstrate the response of the system under wind load or service level of earthquake (SLE).

Stage 2: Sliding on surface 1 and 3 with a decrease in

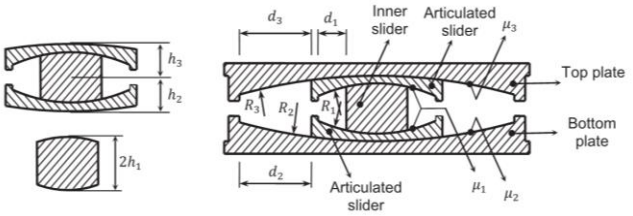

Fig. 1 Section view of Triple Friction Pendulum Bearing (Dao *et al.* 2013)

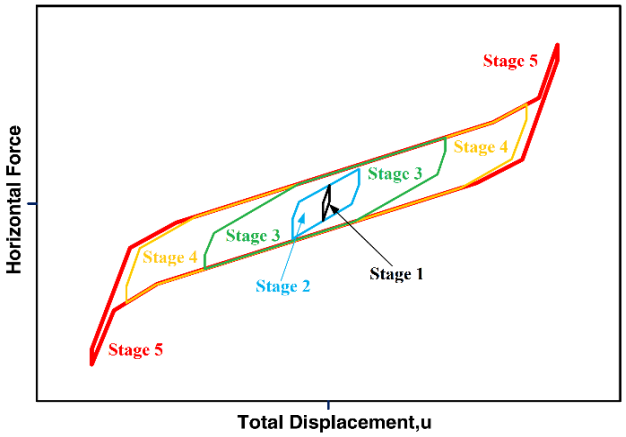

Fig. 2 The five stages of force-displacement behavior of TFPB (Moeindarbari and Taghikhany 2014)

stiffness and friction increase. This stage defines the properties of the isolator during moderate levels of earthquake.

Stage 3: Stopping the motion in surface 2 and 3, followed by sliding on surface 1 and 4.

Stage 4: Reaching of slider to restrainer on surface 1. The sliding occurs on surface 2 and 4.

Stage 5: Bearing of slider on restrainer of surface 1 and 4 while the motion continues by sliding on surface 2 and 3.

It is required that the isolator reaches a certain value of displacement to enter the next sliding stage and change its hysteresis behavior. The stages 3 and 4 show the force-displacement behavior of the isolator against the extreme level of excitation (Maximum considered event or MCE) and it is not preferred that the stage 5 of sliding be activated even under the MCE earthquake level (Morgan and Mahin 2011). A thorough review of the TFPB and its governing equations of force-displacement behavior is represented by Fenz (2008); also the recommended combination of optimized design parameters for the TFPB isolators can be found in Moeindarbari and Taghikhany (2014).

3. Impact modelling

To analyze the effect of impact on the performance of TFPB-isolated building, a 3D symmetrical single story building with rigid floors is considered. Two levels of building's roof (top deck) and base level (bottom deck) are considered for the frame. Fig. 3 shows the frame geometry

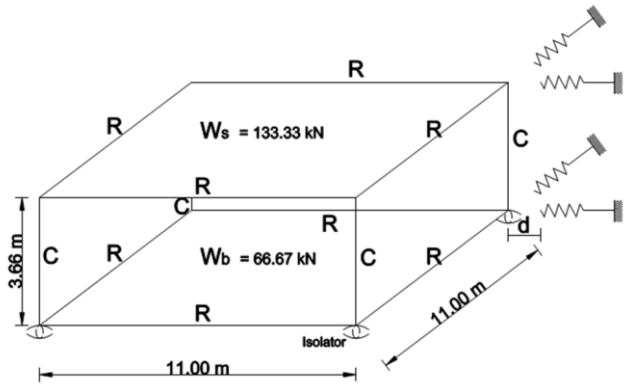

Section Property	Area (mm^2)	Moments of Inertia (mm^4)	Torsion Constant (mm^4)	Shear Area (mm^2)	Mass (kg)	Weight (kN)
"Column" (C)	5.0×10^6	6.851×10^7	1.0×10^8	5.0×10^6	0	0
"Rigid" (R)	5.0×10^6	1.0×10^{11}	1.0×10^8	5.0×10^6	0	0

Fig. 3 The specification of the utilized isolated superstructure

and weights associated to each deck along with its members' geometrical and mechanical properties. The system with fixed base has a damping ratio of 0.25% and period of 0.2 s in both directions. For the numerical modeling of impact, the presence of the adjacent structure is considered by utilizing a linear spring located at a specific distance from the building to capture the amount of pounding force on two levels of the frame. As for the structures without adjacent buildings, the stiffness of the springs can be modified to zero. The amount of impact force imposed to the building can be measured by the spring force. Seismic impact occurs when the absolute bearing displacement at each level exceeds the isolation gap *d* between the isolated building and the adjacent structure, during a seismic excitation. The force-displacement relationship for the generated impact force, with respect to the base deck and building's roof, can be evaluated as

$$F_{rbx} = K_{rb}(|u_{bx}| - d)sign(u_{bx})H(|u_{bx}| - d) \quad (1)$$

$$F_{rsx} = K_{rs}(|u_{sx}| - d)sign(u_{sx})H(|u_{sx}| - d) \quad (2)$$

Where F_{rbx} and F_{rsx} are pounding force applied to the building in base deck and roof level of structure in *x*-direction, respectively. The parameters K_{rb} and K_{rs} represent the stiffness of the adjacent structure in the base deck and top deck, respectively; and d is the distance between the two structures while H(*) denotes the Heaviside step function. The same equations can be obtained for poundings in the *y*-direction; also, the values of K_{rs} and K_{rb} are taken as equal and ten times of the initial stiffness of the isolated structure, respectively. Since the columns are assumed to be massless and the impact forces are imposed only at the both decks, the shear profile for the columns is expected to be uniform; also, it should be noted that the above impact

Table 1 The required parameters for the three SFPB elements to model a TFPB

	Friction coefficient	Radius of curvature	Nominal displacement capacity	Rate parameter
Element 1	$\bar{\mu}_1 = \mu_2 = \mu_3$	$\bar{R}_{eff\,1} = R_{eff\,2} + R_{eff\,3}$	$\bar{d}_1 = (d_1 + d_2 + d_3 + d_4) + (\bar{d}_2 + \bar{d}_3)$	$\bar{a}_1 = \frac{1}{2}\frac{(a_2 + a_3)}{2}$
Element 2	$\bar{\mu}_2 = \mu_1$	$\bar{R}_{eff\,2} = R_{eff\,1} - R_{eff\,2}$	$\bar{d}_2 = \frac{R_{eff\,1} - R_{eff\,2}}{R_{eff\,1}} d_1$	$\bar{a}_2 = \frac{R_{eff\,1}}{R_{eff\,1} - R_{eff\,2}} a_1$
Element 3	$\bar{\mu}_3 = \mu_4$	$\bar{R}_{eff\,3} = R_{eff\,4} - R_{eff\,3}$	$\bar{d}_3 = \frac{R_{eff\,4} - R_{eff\,3}}{R_{eff\,4}} d_4$	$\bar{a}_3 = \frac{R_{eff\,4}}{R_{eff\,4} - R_{eff\,3}} a_4$

modelling only take into accounts the floor-to-floor pounding and other types of pounding such floor-to-column (Karayannis and Favvata 2005a, b) is not considered here.

It is worth mention that TFPB base isolators demonstrate five regimes of motion in their cyclic force-displacement behavior, as stated early in the paper. Normally, the buildings isolated by TFPB are designed in a way that their isolators would be working in the third and fourth regime of motion during a strong seismic excitation. In this paper, the distance between the two structures "d" is assumed to be equal to the displacement of the TFPB in the middle of its third and fourth regime of motion to make sure that the impact would occur when the isolators are working in their third or fourth stage of motion.

4. Equation of motions

To simulate the behavior of the buildings isolated by TFPB, the symmetrical 3D single story frame shown in Fig. 3 was selected as a superstructure, resting on four TFPB base isolators. The weight of columns and beams are assumed to be negligible against the mass of the entire building. Such a model was employed by other researchers such as Fenz and Constantinou (2008a). The building is modelled as an elastic rigid body since the seismically isolated frames are expected to remain elastic during earthquakes. Since the centers of masses of the top and bottom decks are assumed to be vertically aligned, no torsional coupling is expected for the building during analysis. The hysteretic behavior of the TFPBs is simulated by using three Single Friction Pendulum Bearing (SFPB) link acting in series with two small point masses (m_1 and m_2) representing the articulated slider (Fenz and Constantinou 2008a) as shown in Fig 4. Each link is composed of three distinct elements connected in parallel: A linear spring with a stiffness of $\bar{R}_{effi}$, an equivalent friction element with a friction coefficient of $\bar{\mu}_i$ and a gap element, simulating the displacement capacities of the base isolator in each slider. The summary of the parameters needed for modelling the three SFPBs are presented in Table 1.

The horizontal force produced by this arrangement is calculated by

$$F_i = \frac{W}{\bar{R}_{effi}} u_i + \bar{\mu}_i W Z_i + K_i(|u_i| - \bar{d}_i)\,sign(u_i)\,H(|u_i| - \bar{d}_i) \quad (3)$$

Which can be computed in both *x*- and *y*-direction. W is the mass supported by each isolator, u_i is the radial relative displacement of SFPB element, K_i is the stiffness of the displacement restrainer of the TFPB which should be assigned a large value to model the restraining mechanism. Z_{ix} and Z_{iy} can be approximately expressed by solving the following differential matrix

$$Y\begin{Bmatrix}\dot{Z}_{ix}\\ \dot{Z}_{iy}\end{Bmatrix} = A\begin{bmatrix}1 & 0\\ 0 & 1\end{bmatrix}\begin{Bmatrix}\dot{u}_{ix}\\ \dot{u}_{iy}\end{Bmatrix} - \begin{bmatrix}|Z_{ix}|^2[\gamma sign(\dot{u}_{ix}Z_{ix}) + \beta] & Z_{ix}Z_{iy}[\gamma sign(\dot{u}_{ix}Z_{ix}) + \beta]\\ Z_{ix}Z_{iy}[\gamma sign(\dot{u}_{iy}Z_{iy}) + \beta] & |Z_{iy}|^2[\gamma sign(\dot{u}_{iy}Z_{iy}) + \beta]\end{bmatrix}\begin{Bmatrix}\dot{u}_{ix}\\ \dot{u}_{iy}\end{Bmatrix} \quad (4)$$

Where A, β and γ are dimensionless variables that control the shape of the hysteretic loop with a constant value of 1, 0.9 and 1, respectively (Amiri and Namiranian 2014); The parameter Y is the yield displacement of the sliding surfaces, which is taken as 0.25 mm in this study, and sign denotes the signum function.

The sliding friction coefficients of the isolator are modeled as the velocity-dependent coefficients of friction using the equation below

$$\bar{\mu}_i = \mu_{\max} - (\mu_{\max} - \mu_{\min})e^{-a|\dot{u}_i|} \quad (5)$$

Where $\mu_{\max}$ and $\mu_{\min}$ represent the coefficient of friction at high and very low velocities, respectively. The rate parameter a controls the variation between the lowerbound and upperbound values of μ, and $\dot{u}_i$ is the

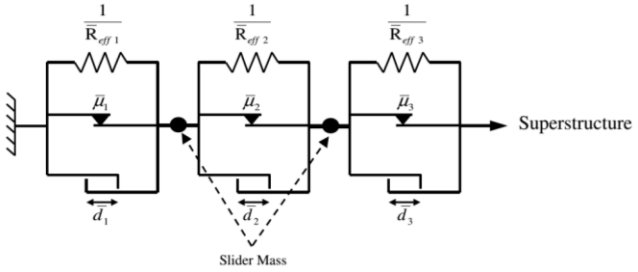

Fig. 4 Three Friction Pendulum linked in series to model TFPB (Amiri and Namiranian 2015)

radial sliding velocity of ith SFPB element ($\dot{u}_i = \sqrt{\dot{u}_{ix}^{\ 2} + \dot{u}_{iy}^{\ 2}}$).

The dynamic behavior of the system can be expressed by designating eight degrees of freedom as follows:

u_{sx} and u_{sy} are used to record the displacement of the building in top deck while u_{bx} and u_{by} are employed for recording the bottom deck movement (four degrees in total). Also, each mass slider possesses bi-directional movements in x- and y-axis, which indicates that four degrees of freedom are needed to calculate the response of the base isolator during a seismic excitation (Fig. 5).

The equations of motion of the system subjected to the seismic excitation in the x-direction can be calculated as

$$\begin{bmatrix} m_s & 0 & 0 & 0 \\ 0 & m_b & 0 & 0 \\ 0 & 0 & m_2 & 0 \\ 0 & 0 & 0 & m_1 \end{bmatrix} \begin{Bmatrix} \ddot{u}_{sx} \\ \ddot{u}_{bx} \\ \ddot{u}_{2x} \\ \ddot{u}_{1x} \end{Bmatrix} + \begin{bmatrix} C_{sx} & -C_{sx} & 0 & 0 \\ -C_{sx} & C_{sx} & 0 & 0 \\ 0 & 0 & 0 & 0 \\ 0 & 0 & 0 & 0 \end{bmatrix} \begin{Bmatrix} \dot{u}_{sx} \\ \dot{u}_{bx} \\ \dot{u}_{2x} \\ \dot{u}_{1x} \end{Bmatrix} +$$

$$\begin{bmatrix} K_{sx} & -K_{sx} & 0 & 0 \\ -K_{sx} & K_{sx} & 0 & 0 \\ 0 & 0 & 0 & 0 \\ 0 & 0 & 0 & 0 \end{bmatrix} \begin{Bmatrix} u_{sx} \\ u_{bx} \\ u_{2x} \\ u_{1x} \end{Bmatrix} \tag{6}$$

$$= -\begin{bmatrix} m_s & 0 & 0 & 0 \\ 0 & m_b & 0 & 0 \\ 0 & 0 & m_2 & 0 \\ 0 & 0 & 0 & m_1 \end{bmatrix} \begin{bmatrix} 1 & 0 & 0 & 0 \\ 0 & 1 & 0 & 0 \\ 0 & 0 & 1 & 0 \\ 0 & 0 & 0 & 1 \end{bmatrix} \ddot{u}_{gx} - \begin{Bmatrix} F_{rsx} \\ F_{rbx} + F_{1x} \\ F_{2x} - F_{1x} \\ F_{3x} - F_{2x} \end{Bmatrix}$$

Where m_1 and m_2 are the small masses assigned to the slider, K_{SX} and C_{SX} are the stiffness and damping coefficient of the superstructure in the x-direction, respectively; $\ddot{u}_{gx}$ is the x-component of the ground acceleration; and F_{ix} is the force in the ith SFPB element along the x-direction. F_{rsx} and F_{rbx} are the impact forces which were defined previously. The same equations can be written for the y-direction.

By rearranging the above equations, the equation of motions for the system can be written as

$$\{\dot{x}\} = [A]\{x\} + \{B\} \tag{7}$$

Where the vector $\{x\}$ is

$$\{x\} = \{u_{m1x} \quad u_{m1y} \quad u_{m2x} \quad u_{m2y} \quad u_{bx} \quad \dot{u}_{bx} \quad \dot{u}_{by} \quad \dot{u}_{sx} \quad \dot{u}_{sy} \quad Z_{1x} \quad Z_{1y} \quad u_{by} \quad u_{sx} \quad u_{sy} \quad \dot{u}_{m1x} \quad \dot{u}_{m1y} \quad \dot{u}_{m2x} \quad \dot{u}_{m2y} \quad Z_{2x} \quad Z_{2y} \quad Z_{3x} \quad Z_{3y}\}^T. \tag{8}$$

The above ordinary differential equations are solved simultaneously by using the ode15s solver in MATLAB. The ode15s solver is a variable order, multi-step algorithm that is efficient for solving systems of stiff differential equations.

To verify the equations and validate our code, the result tests extracted by Fenz and Constantinou (2008a) were utilized and the same base-isolated structure were developed analytically. Fig 6 compares our results with the numerical outcomes reported by Fenz and Constantinou.

5. Ground motion records and isolators' description

5.1 Selection of ground motion records

To investigate the performance TFPB isolation systems, a suite of seven pairs of near-fault ground motion records is selected to perform nonlinear time history analysis. The records are downloaded from the PEER ground motion database (Table 2) and cover a magnitude range of 6.6~7.4. It should be noted that five pairs of the records are among the pulse-like earthquakes while the remaining two earthquakes are non-pulse like motions. For simplicity, only the horizontal components of the records (fault-normal and fault-parallel) are considered for analysis, due to the negligible influence of the vertical excitations of the earthquake records on the isolation's displacement response (Fenz 2008, Fadi and Constantinou 2010).

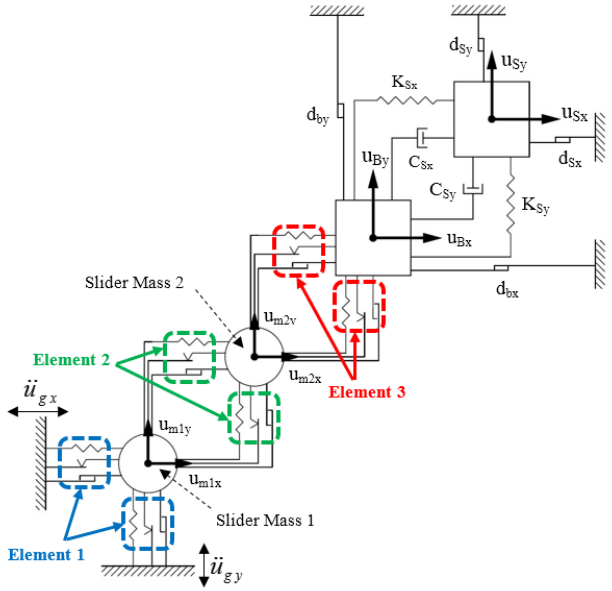

Fig. 5 Mathematical model of 3D single-story structure on TFPB with considering impact on two level of top and bottom deck

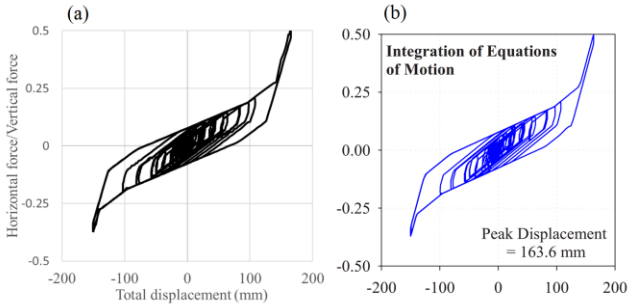

Fig. 6 Comparison of TFPB force-displacement from (a) our results and (b) results from Fenz and Constantinou (2008a)

Table 2 Selected ground motion records for analysis (* denotes non-pulse ground motions)

Seismic Event	Year	Station Name	M_w	Component	PGA (g)	PGV (cm/s)	PGD (cm)
Bam	2003	Bam	6.6	Normal	0.81	124.1	33.9
				Parallel	0.63	60.2	23.2
Cape Mendocino	1992	Petrolia	7	Normal	0.59	81.9	25.5
				Parallel	0.66	60.4	26.0
Turkey Erzincan*	1992	Erzincan	6.7	Normal	0.52	107.1	32.0
				Parallel	0.5	78.2	28.0
Kobe	1995	Takaraz uka	6.9	Normal	0.69	86.3	20.8
				Parallel	0.69	68.4	26.7
Northridge	1994	Newhall	6.7	Normal	0.58	120.1	35.1
				Parallel	0.59	49.9	16.2
Northridge*	1994	Sylmar	6.7	Normal	0.60	130.3	54.0
				Parallel	0.84	93.3	53.3
Tabas	1978	Tabas	7.4	Normal	0.85	118.3	96.8
				Parallel	0.86	79.6	42.1

5.2 Isolators' description

To investigate the performance of TFPB isolation systems, a set of 20 TFPB, similar to the ones designed by Amiri *et al.* (2015) were used. These isolation systems include five groups of TFPB with different geometric configurations which consider four different cases of friction coefficient for each group. Tables 3 and 4 provides a summary of the geometric configurations and friction coefficients for the isolators. The GC1 corresponds to the smallest modelled isolator while GC5 denotes the largest TFPB in terms of physical measures. Also, the friction coefficient LF, MF and HF represent the isolation systems with low, moderate and high friction coefficient, respectively. The case EF aims to consider simpler configuration for isolation systems where friction coefficients are taken equal to attain simpler hysteretic behavior. It should be pointed out that as stated by Fenz (2008), in order to achieve all the five sliding fazes in the TFPB isolators, the friction coefficients of the surfaces must be selected such that $\mu_2=\mu_3<\mu_1<\mu_4$ to ensure the full adaptivity of the isolation systems. However, in case of friction coefficient EF ($\mu_1=\mu_4$), the force-deformation behavior of the isolator will collapse to double friction pendulum systems where the isolator provides only three stages of motion. The reason is that when the friction is equal on two surfaces *i* and *j*, sliding occurs simultaneously on both surfaces and they act as a single surface. As for the other cases (LF, MF and HF) the isolation system works in its fully adaptive configuration which is capable of presenting all the five regimes of motion.

The separation distances for the isolators are provided in the table 5. As for the isolators with friction coefficients of LF, MF and EF, two different values are selected to investigate the impact while the isolator is working in its third and fourth regime of motion. To do so, the minimum and maximum displacement capacity of the isolator in its third sliding stage is evaluated and the average value is computed for the gap. The similar calculations are conducted for the fourth regime of motion to ensure that the impact would occur in the isolator's fourth sliding stage.

Table 3 Geometry configuration of the TFPB models

Isolator Groups	Displacement capacities (mm)			Effective radius (mm)	
	$d_2=d_3$	$d_1=d_4$	d_{TOT}	$R_{eff2}=R_{eff3}$	$R_{eff1}=R_{eff4}$
GC1	30	100	260	150	750
GC2	65	180	490	355	1500
GC3	65	180	490	495	2085
GC4	85	190	550	700	3000
GC5	110	230	680	900	3825

Table 4 Friction coefficient cases in each group of TFPB

Case	$\mu_2=\mu_3$	μ_1	μ_4	μ_2:μ_1:μ_4
LF	0.02	0.04	0.10	1:2:5
MF	0.02	0.06	0.12	1:3:6
HF	0.02	0.08	0.14	1:4:7
EF	0.02	0.08	0.08	1:4:4

Table 5 Separation distance values for each building model (in mm)

	GC1		GC2		GC3		GC4		GC5	
Regime	III	IV	III	IV	III	IV	III	IV	III	IV
LF	115	197	216	361	229	361	260	381	320	462
MF	121	203	230	375	249	381	288	409	356	498
HF	127	209	244	390	269	401	316	437	392	534
EF	118		223		239		274		338	

6. Analysis results

The modelled structures were subjected to the seven pairs of earthquake ground motion and the results are evaluated in terms of roof acceleration, base shear demands and drift ratio of the superstructure. The maximum amount of each parameter is evaluated during the time history analysis for the seven earthquake records and the average value is presented for each isolated-structure. Also, the effect of impact element stiffness on the response of isolated buildings is investigated.

6.1 The effect of impact on the roof acceleration of TFPB-isolated buildings

Fig. 7 presents the average of maximum roof acceleration demand in each earthquake record for the isolated buildings. As can be seen, for the isolators GC1, GC2 and GC3 the acceleration values for the buildings without seismic pounding is larger than the buildings who experience pounding while the isolator is in sliding stage 3 or 4. As for the GC4 isolators, the acceleration value is

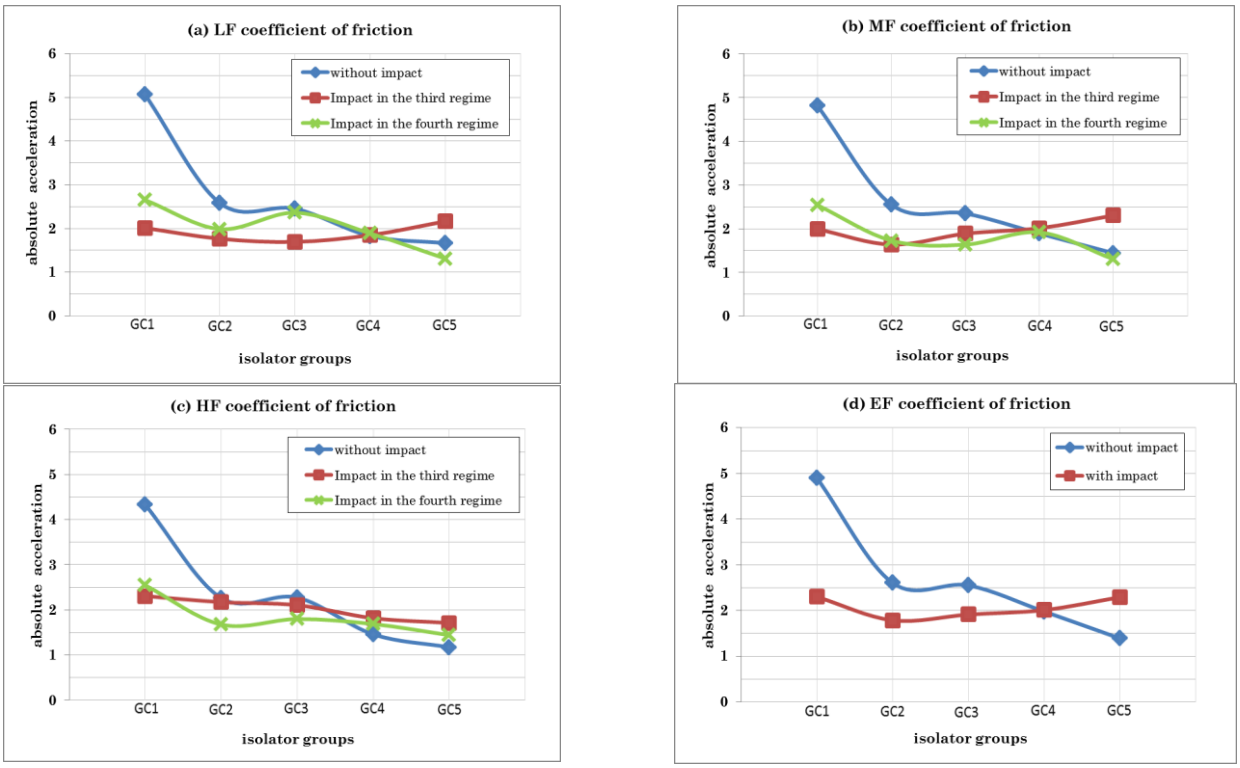

Fig. 7 Comparison of roof acceleration demands (in m/s^2) for isolated frames considering the effects of impact

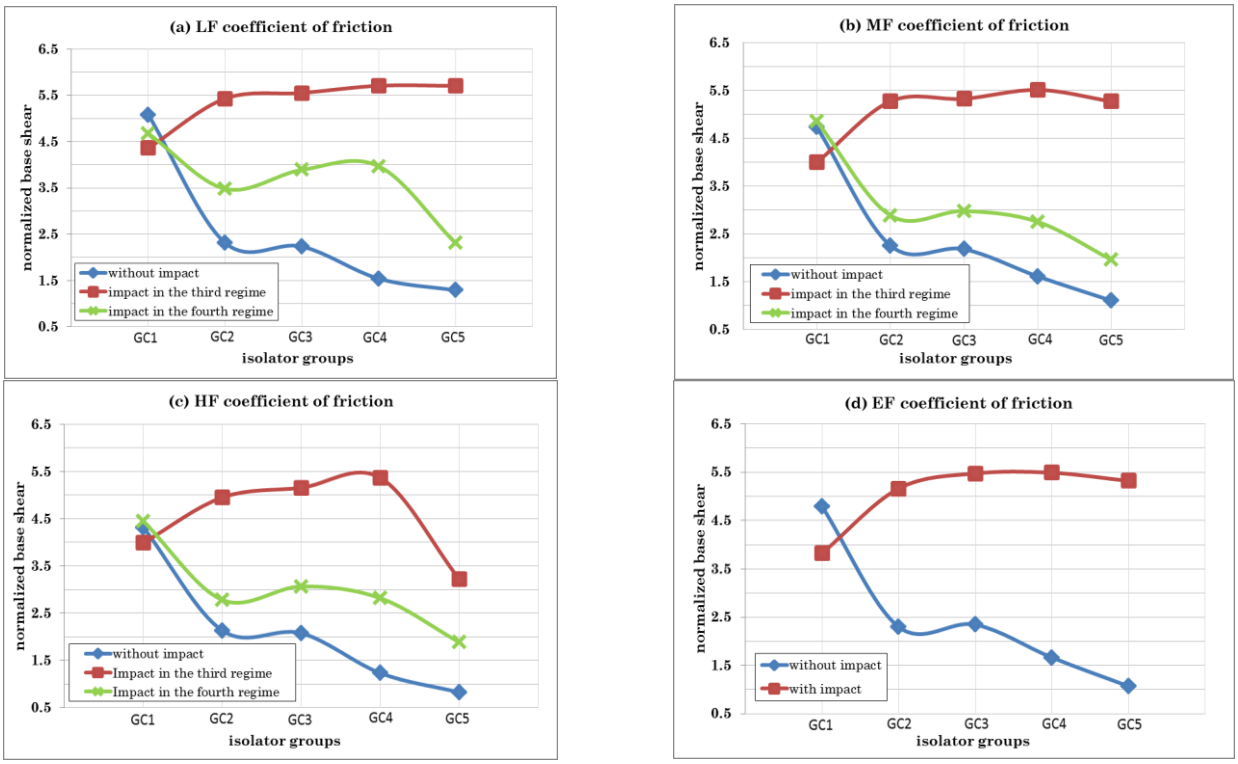

Fig. 8 Comparison of seismic base shear demands for isolated frames considering the effects of impact

nearly equal for the buildings with or without seismic pounding; however, the effect of impact on roof acceleration demands tends to intensify for isolators with bigger dimensions, especially the ones who tolerate the pounding in their third regime of motion. The highest increment due to impact was witnessed for GC5-MF isolator in its third sliding stage where the acceleration increased nearly 60% as compared to the same system without pounding. Another fact is that although increasing the isolator dimension normally elevates the fundamental

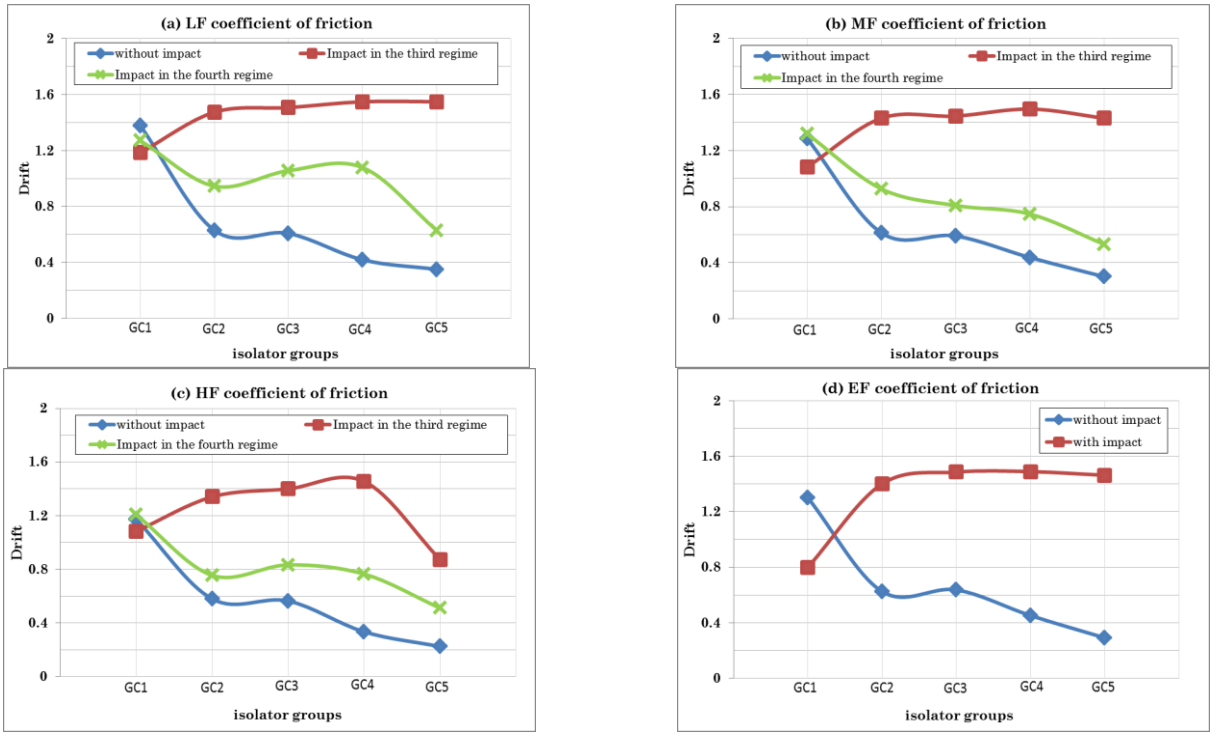

Fig. 9 Comparison of interstory drift demands for isolated frames considering the effects of impact

period of the overall system which results in lower acceleration demands in the superstructure, it does not influence the acceleration significantly in case of pounding occurrence. This would mean that utilizing TFPBs with higher fundamental periods does not necessarily lowers the acceleration demand on superstructures and a sufficient gap is needed to ensure the proper functioning of the isolation system.

6.2 The effect of impact on the base shear of TFPB-isolated buildings

Fig. 8 demonstrates the effect of seismic pounding on base shear demands of the structures resting on the TFPB systems. The shear forces are normalized by the total superstructure weight. As can be seen, the seismic impact increases the shear forces in the superstructure and the level of increment is higher in case of isolation systems which tolerate seismic impact in their third sliding stage. It can be concluded that in case of pounding occurrences in the adjacent buildings, the size of separation distance can adversely affect the base shear demand since the impact in the third sliding stage of a TFPB (with smaller gap) causes higher base shear than impact in the fourth stage of a same system. The highest value for the average base shear increment was recorded at nearly 500% for GC5-EF isolator, 480% for GC5-MF in its third regime and 257% for GC4-LF isolator in its fourth regime of motion.

Albeit, it can be seen that the seismic pounding lowered the base shear demands for the GC1 isolation group. This behavior is due to the limited displacement capacity of the GC1 isolators as compared to other isolation groups with bigger geometric configuration. Moreover, it can be seen that selecting bigger isolation systems with larger values of the fundamental period tends to alleviate the pounding-induced shear demands of the structure. However, it is also necessary to utilize higher friction coefficients for sliding surfaces of the isolation systems which experience impact in their third regime of motion.

6.3 The effect of impact on the drift demands of TFPB-isolated buildings

The maximum drift ratio of the superstructure was calculated during the time history analyses and the average values are calculated for each isolation group and depicted in Fig. 9. By comparison with the figure given for the base shear demands of the building, a similar pattern could be identified which shows the direct relation between base shear and drift ratio of the superstructure. The horizontal pounding force imposed to the superstructure would also increase the drift demands, and since the impact forces are more severe in case of occurring impact in the third regime of the isolator motion, the average drift values are higher in this case, as compared to the other two cases. Moreover, selection of isolation systems with higher fundamental period would decrease the drift demands on the superstructure; however, for the isolators which experience seismic pounding in their third regime of motion, the friction coefficient of the sliding surfaces should also be increased to lower the pounding-induced drift more effectively.

6.4 The effect of adjacent structures' stiffness on impact

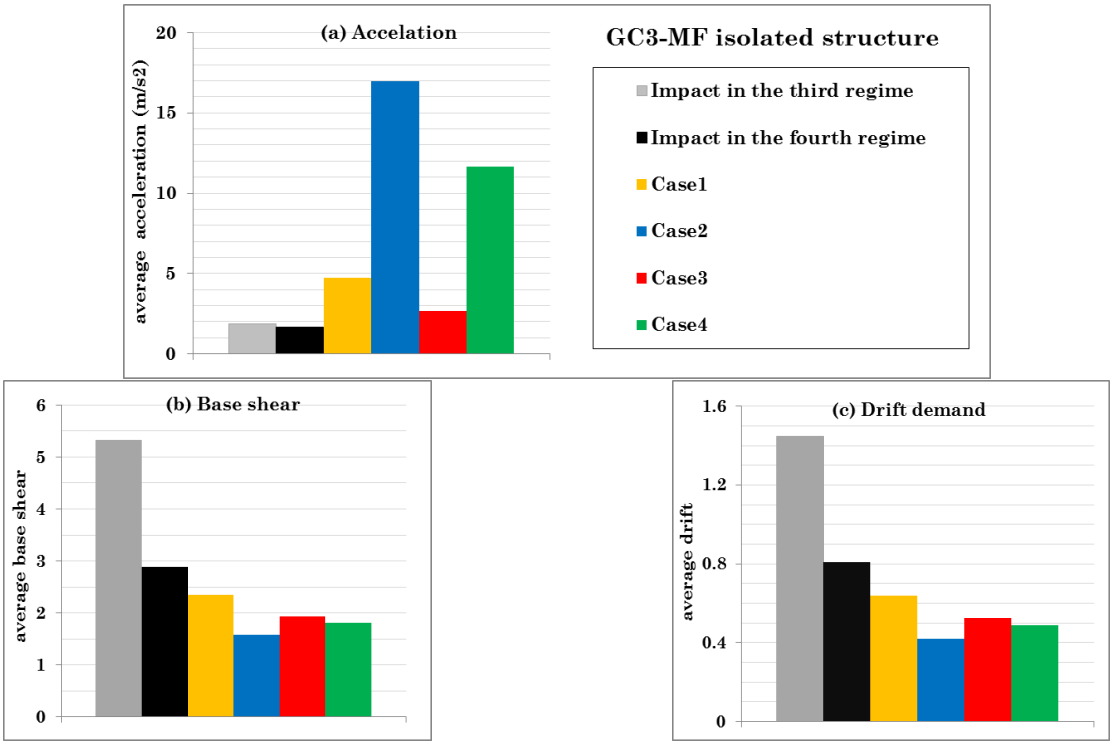

Fig. 10 Effect of impact element stiffness on the (a) acceleration, (b) normalized base shear, and (c) drift demands of the superstructure

To estimate the impact forces applying on the colliding structures, a set of impact elements characterized by linear springs located at the gap distance *d* from the superstructure were employed on both top deck and bottom deck of the isolated building. The previous results were based on an assumption that the stiffness of the impact element would be equal and ten times of the superstructure stiffness in the top deck and base deck, respectively. In other words

$$\frac{K_{impact}(top)}{K_{impact}(bottom)} = \frac{1S}{10S}, \text{ S: Superstructure stiffness} \quad (9)$$

While pounding occurs in the third and fourth sliding stages of isolation systems. In this part, four other cases are considered for the impact element stiffness on the two levels of base and top deck:

Case 1: $\frac{K_{impact}(top)}{K_{impact}(bottom)} = \frac{1S}{1S}$ (flexible) and impact would occur in the **third** regime of motion.

Case 2: $\frac{K_{impact}(top)}{K_{impact}(bottom)} = \frac{10S}{10S}$ (rigid) and impact would occur in the **third** regime of motion.

Case 3: $\frac{K_{impact}(top)}{K_{impact}(bottom)} = \frac{1S}{1S}$ (flexible) and impact would occur in the **fourth** regime of motion.

Case 4: $\frac{K_{impact}(top)}{K_{impact}(bottom)} = \frac{10S}{10S}$ (rigid) and impact would occur in the **fourth** regime of motion.

Fig. 10 presents the obtained results for the GC3-MF isolated building which denotes the system with medium friction coefficient and intermediate physical dimensions. As can be seen from the graph, the acceleration demands on the superstructure tend to increase when equal stiffness is selected for the impact elements on top and bottom deck levels. Also, the accelerations are higher for the more rigid adjacent structure as the results for the cases 2 and 4 are nearly four times bigger than the flexible cases 1 and 3. Moreover, a similar pattern is witnessed for the base shear and drift demands of the superstructure which highlights the direct relation between the two parameters. The obtained results show that selecting higher value for stiffness on the top deck impact element reduces the drift ratio of the superstructure which also results in a less base shear demands. This can show that besides the stiffness of the adjacent building, the results of the seismic-induced pounding shear forces are also dependent on the distribution of the impact element stiffness; and more accurate models are needed to sufficiently consider the stiffness of the adjacent structures on each story level.

7. Conclusions

In this paper, a detailed numerical investigation was conducted using nonlinear dynamic time history analyses to investigate the performance of TFPB base isolation systems during seismic impact by considering different friction coefficient and geometric configurations. Based on the calculated results, the following major conclusions can be

drawn:

- As the fundamental period of base isolators increases, one could expect the decrement of the seismic base shear in buildings. However, with the effects of impact of adjacent structures, the base shear demands increases. It is worth mention that base shear changes are larger when the TFPB isolation systems are within their third regime of motion, as compared to the fourth regime. The highest value for base shear increment was calculated at 480% and 257% higher than isolated buildings without impact effects, for fully adaptive base isolators which tolerate impact in their third and fourth regime of motion, respectively.
- Impact caused larger drift demands as compared to the buildings without pounding effects. The highest value of drift was computed five time higher in the isolation systems with earthquake impact, as compared to the structure without any adjacent building.
- By increasing the geometric configuration of the TFPBs, the fundamental period of the base isolator increases which results in a decrement in the superstructure's base shear for the buildings without pounding effects and isolated buildings tolerating pounding effects in their fourth stages of motion. However, a different trend is witnessed in case of isolation systems with pounding in their third regime of motion and it is required to increase the displacement capacities of the isolator as well as its friction coefficient to lower the seismic pounding shear demands.
- By investigating various cases for the impact element stiffness in the top and bottom story levels of the superstructure, it has been found that the different distribution patterns of stiffness on story levels of adjacent building has a decisive role in the estimation of the impact force imposed on TFPB isolation systems.

It should be pointed out that the present paper utilized an elastic single story building to investigate the effects of seismic pounding on the performance of TFPB isolation systems and does not assess the local effects such as the effects of inter-story pounding, ductility demands and the effects of pounding area. A number of parameters and modelling assumption could influence the overall response of the building such as the number of stories and the effects of infilled panels (Karayannis *et al.* 2011). Although the utilized model can reasonably evaluate the base isolator's performance during seismic pounding, more developed analytical models are required to investigate the performance of the superstructure during impact. Also, more advanced models should be employed to simulate the pounding effects of the adjacent buildings with consideration of the impact elements stiffness distribution along the entire height of the isolated MDOF structure.

References

Amiri, G.G. and Namiranian, P. (2014), "Evaluation of capacity spectrum method in estimating seismic demands of triple pendulum bearings under near-field ground motions", *Int. J. Struct. Stab. Dyn.*, **14**(02), 1350062.

Amiri, G.G., Namiranian, P. and Amiri, M.S. (2015), "Seismic Response of Triple Friction Pendulum Bearing under Near-Fault Ground Motions", *Int. J. Struct. Stab. Dyn.*, **16**(06), 1550021.

Anagnostopoulos, S.A. (1988), "Pounding of buildings in series during earthquakes", *Earthq. Eng. Struct. Dyn.*, **16**(03), 443-456.

Bertero, V.V. (1987), "Observations on structural pounding", *Proceedings of The Mexico Earthquakes-1985: Factors Involved and Lessons Learned*, Mexico City, Mexico, September.

Cole, G., Dhakal, R., Carr, A. and Bull, D. (2011), "Case studies of observed pounding damage during the 2010 Darfield earthquake", *Proceedings of the 9th Pacific Conference on Earthquake Engineering Building an Earthquake-Resilient Society*, Auckland, New Zealand, April.

Dao, N.D., Ryan, K.L., Sato, E. and Sasaki, T. (2013), "Predicting the displacement of triple pendulum™ bearings in a full-scale shaking experiment using a three-dimensional element", *Earthq. Eng. Struct. Dyn.*, **42**(11), 1677-1695.

Fadi, F. and Constantinou, M.C. (2010), "Evaluation of simplified methods of analysis for structures with triple friction pendulum isolators", *Earthq. Eng. Struct. Dyn.*, **39**(1), 5-22.

Fenz, D.M. (2008), "Development, implementation and verification of dynamic analysis models for multi-spherical sliding bearings", Ph.D. Dissertation, University of Buffalo, New York.

Fenz, D.M. and Constantinou, M.C. (2008a), "Modeling triple friction pendulum bearings for response-history analysis", *Earthq. Spectra*, **24**(4), 1011-1028.

Fenz, D.M. and Constantinou, M.C. (2008b), "Spherical sliding isolation bearings with adaptive behavior: Theory", *Earthq. Eng. Struct. Dyn.*, **37**(2), 163-183.

Karayannis, C.G. and Favvata, M.J. (2005a), "Earthquake-induced interaction between adjacent reinforced concrete structures with non-equal heights", *Earthq. Eng. Struct. Dyn.*, **34**(1), 1-20.

Karayannis, C.G. and Favvata, M.J. (2005b), "Inter-story pounding between multistory reinforced concrete structures", *Struct. Eng. Mech.*, **20**(5), 505-526.

Karayannis, C.G., Favvata M.J. and Kakaletsis D.J. (2011), "Seismic behaviour of infilled and pilotis RC frame structures with beam-column joint degradation effect", *Eng. Struct.*, **33**(10), 2821-2831.

Kasai, K. and Maison, B.F. (1997), "Building pounding damage during the 1989 Loma Prieta earthquake", *Eng. Struct.*, **19**(3), 195-207.

Khoshnoudian, F. and Hemmati, T.A. (2014), "Impact of structures with double concave friction pendulum bearings on adjacent structures", *Proceedings of the Institution of Civil Engineers-Structures and Buildings*, **167**(1), 41-53.

Komodromos, P., Polycarpou, P.C., Papaloizou, L. and Phocas, M.C. (2007), "Response of seismically isolated buildings considering poundings", *Earthq. Eng. Struct. Dyn.*, **36**(12), 1605-1622.

Mahmoud, S., Abd-Elhamed, A. and Jankowski, R. (2013), "Earthquake-induced pounding between equal height multi-storey buildings considering soil-structure interaction", *Bull. Earthq. Eng.*, **11**(4), 1021-1048.

Malhotra, P.K. (1997), "Dynamics of seismic impacts in base-isolated buildings", *Earthq. Eng. Struct. Dyn.*, **26**(8), 797-813.

Masroor, A. and Mosqueda, G. (2012), "Experimental simulation of base-isolated buildings pounding against moat wall and effects on superstructure response", *Earthq. Eng. Struct. Dyn.*, **41**(14), 2093-2109.

Matsagar, V.A. and Jangid, R. (2003), "Seismic response of base-isolated structures during impact with adjacent structures", *Eng.*

Struct., **25**(10), 1311-1323.
Moeindarbari, H. and Taghikhany, T. (2014), "Seismic optimum design of triple friction pendulum bearing subjected to near-fault pulse-like ground motions", *Struct. Multidisciplin. Optimiz.*, **50**(4), 701-716.
Morgan, T.A. and Mahin, S.A. (2011), "The use of base isolation systems to achieve complex seismic performance objectives", Pacific Earthquake Engineering Research Center, Berkley, California, U.S.A.
Namiranian, P., Amiri, G.G. and Veismoradi, S. (2016), "Near-fault seismic performance of triple variable friction pendulum bearing", *J. Vibro Eng.*, **18**(4), 2293-2303.
Polycarpou, P.C. and Komodromos, P. (2010), "Earthquake-induced poundings of a seismically isolated building with adjacent structures", *Eng. Struct.*, **32**(7), 1937-1951.
Polycarpou, P.C. and Komodromos, P. (2011), "Numerical investigation of potential mitigation measures for poundings of seismically isolated buildings", *Earthq. Struct.*, **2**(1), 1-24.
Polycarpou, P.C., Komodromos, P. and Polycarpou, A.C. (2013), "A nonlinear impact model for simulating the use of rubber shock absorbers for mitigating the effects of structural pounding during earthquakes", *Earthq. Eng. Struct. Dyn.*, **42**(1), 81-100.
Raheem, S.E.A. (2014), "Mitigation measures for earthquake induced pounding effects on seismic performance of adjacent buildings", *Bull. Earthq. Eng.*, **12**(4), 1705-1724.
Rawlinson, T.A., Marshall, J.D., Ryan, K.L. and Zargar, H. (2015), "Development and experimental evaluation of a passive gap damper device to prevent pounding in base-isolated structures", *Earthq. Eng. Struct. Dyn.*, **44**(11), 1661-1675.
Takewaki, I., Murakami, S., Fujita, K., Yoshitomi, S. and Tsuji, M. (2011), "The 2011 off the Pacific coast of Tohoku earthquake and response of high-rise buildings under long-period ground motions", *Soil Dyn. Earthq. Eng.*, **31**(11), 1511-1528.

AT